Version 4.02

Spectroscopic study of Λ hypernuclei up to medium-heavy mass region through the (e,e'K^+) reaction

(Update to the conditionally approved E97-008)

O. Hashimoto (Spokesperson)*, S.N. Nakamura (Spokesperson), Y. Fujii, H. Tamura, T. Takahashi, K. Maeda, H. Kanda, T. Miyoshi, H. Yamaguti, Y. Okayasu, K. Tsukada

Department of Physics, Tohoku University, Sendai, 980-8578, Japan

S. Kato

Department of Physics, Yamagata University, Yamagata, 990-8560, Japan

H. Noumi

Institute for Particle and Nuclear Physics, KEK, Tsukuba, 305-0801, Japan

T. Motoba

Laboratory of Physics, Osaka Electro-Communication University, Neyagawa, 572-8530, Japan

L. Tang (Spokesperson), O.K. Baker, L. Cole, M. Christy, L. Gan, A. Gasparian, P. Gueye, B. Hu, C. Jackson, C. Keppel, Y. Sato, A. Uzzle, L. Yuan, X.F. Zhu

Department of Physics, Hampton University, Hampton, VA 23668, USA

J. Reinhold (Spokesperson), P. Markowiz

Department of Physics, Florida International University, Miami, FL 27411 USA

Ed. V. Hungerford, K. Lan, G.H. Xu

Department of Physics, University of Houston, Houston, TX 77204 USA

R. Carlini, R. Ent, H. Fenker, K. Garrow, D. Mack, G. Smith, W. Vulcan, S. Wood, C. Yan

Thomas Jefferson National Accelerator Facility, Newport News, VA 23606 USA

A. Ahmidouch, S. Danagoulian

Department of Physics, North Carolina A& T State University, Greensboro, NC 27411 USA

D. Dehnhard, H. Jungust, J. Liu

Department of Physics, University of Minnesota, Minnesota, USA

N. Simicevic, S. Wells

Department of Physics, Louisiana Tech University, Ruston, LA USA

M. Elaasar

Department of Physics, Southern University at New Orleans, New Orleans, Louisiana, USA

R. Asaturyan, H. Mkrtchyan, A. Margaryan, S. Stepanyan, V. Tadevosyan

Yerevan Physics Institute, Armenia

D. Androic, M. Planinic, M. Furic

Department of Physics, University of Zagreb, Croatia

T. Angelescu

Department of Physics, University of Bucharest, Bucharest, Romania

V. P. Likhachev

Department of Physics, University of Sao Paulo, Sao Paulo, Brasil

December 14, 2000

* Contact person

Osamu Hashimoto

Department of Physics, Tohoku University, Sendai, 980-8578, Japan
hashimot@lambda.phys.tohoku.ac.jp
Telephone 81-22-217-6452
Fax 81-22-217-6455

Proposal to JLAB PAC-19

Abstract

We propose to perform a spectroscopic study of Λ hypernuclei for wide mass region using the (e,e'K^+) reaction. The expected results will provide Λ hypernuclear spectra with the best energy resolution ($\sim$ 300 keV) ever achieved. An energy resolution of a few hundred keV and high statistical accuracy of the level structure will yield knowledge on the single-particle behavior of a Λ hyperon in a medium mass nuclear system, and allow precise studies of the effective Λ-N interaction. The experiment will take full advantage of high quality electron beam at Jlab by introducing a new experimental geometry and a high resolution kaon spectrometer system now under construction.

The (e,e'K^+) reaction has unique characteristics as outlined below.

- A proton is converted to a Λ hyperon.
- Spin-stretched states are populated with both spin-flip and spin-non-flip amplitude.
- Reaction spectroscopy with resolution as good as 300 keV (FWHM) can be realized.

The proposed experiment has two goals,

1. Excitation spectra of medium-heavy Λ hypernuclei will be studied using the ^{28}Si(e,e'K^+)$^{28}_{\Lambda}$Al and ^{51}V(e,e'K^+)$^{51}_{\Lambda}$Ti reactions. This will provide precision binding energies and widths for the Λ hyperon in its various states in nuclear mass up to A=50. The new structures and/or spin-orbit splittings suggested by the recent (π^+, K^+) reaction spectrum in the medium-heavy hypernuclei can be fully investigated with unprecedented energy resolution.
2. Precision measurement of ^{12}C(e,e'K^+)$^{12}_{\Lambda}$B will be used in order to study the detailed structure of a typical *p*-shell Λ hypernucleus in a qualitative way. In particular, the precision spectrum of $^{12}_{\Lambda}$B can be compared to its the mirror symmetric hypernuclei, $^{12}_{\Lambda}$C, which was studied with high statistics but limited resolution by the (π^+, K^+) reaction.

This experiment can now be undertaken with some confidence due to the pioneering and successful E89-009 experiment, completed in the spring of 2000. We have made a through examination of this experiment, and propose a new experimental geometry for the (e,e'K^+) reaction. This geometry will reduce the bremsstrahlung count-rate in the electron spectrometer, which limited the production rate in the experiment, while preserving the resolution and increasing the signal rate. To increase the coincidence rate and improve the resolution a new high-resolution, large-acceptance kaon spectrometer (HKS) is under construction to replace the SOS spectrometer which was used in E89-009.

This proposed experiment will be the first of the series of studies we would intend to undertake using the new kaon spectrometer.

1 Physics Motivation and Experimental Objectives

1.1 Significance of hypernuclear investigation

A hypernucleus contains a hyperon implanted as an "impurity" within the nuclear medium. This introduces a new quantum number, strangeness, into the nucleus, and if the hyperon maintains its identity it will not experience Pauli-blocking, easily interacting with deeply bound nucleons. In this sense, it has been proposed that the hyperon is a good probe of the interior of a nucleus, where information is difficult to obtain.

In the proposed experiment, we intend to extract the characteristics of a Λ hyperon embedded in a nucleus by observing the spectroscopy of its states. It is a unique characteristic of Λ hypernuclei that deeply bound states, even the ground $s-shell$ states, have very small widths and can be measured as individual peaks in the excitation spectra. These properties have, to some extent, been shown experimentally in recent hypernuclear spectroscopy by the (π^+, K^+) reaction[1, 2, 3].

In hypernuclear production, most of the states are excited as nucleon-hole Λ-particle states, $(\mathrm{N}^{-1},\Lambda)$. The spreading widths of these states were calculated to be less than a few 100 keV [4, 5]. This occurs because: 1) The Λ isospin is 0 and only isoscaler particle-hole modes of the core nucleus are excited; 2) the ΛN interaction is much weaker than the nucleon-nucleon interaction; 3) the ΛN spin-spin interaction is weak and therefore the spin vector p_N-h_N excitation is suppressed; and 4) There is no exchange term.

As a result, particle-hole Λ-hypernuclear states are much narrower than nucleon-nuclear states of the same excitation energy. In the case of Ca for example, it was predicted that $\Gamma_\Lambda(1\mathrm{s\ or\ 0d})/\Gamma_N(0\mathrm{s}) = 0.03\text{-}0.07$, resulting in a spreading width narrower than a few hundred keV even for the excited states above the particle emission threshold. This shows that spectroscopic studies of deeply bound Λ-hypernuclear states can be successfully undertaken. Thus through the widths and excitation energies of the single particle levels, the validity of the mean field description of hypernuclear potentials can be examined.

There is also the fundamental question, "to what extent does a Λ hyperon keep its identity as a baryon inside a nucleus?" [6]. Spectroscopic data in heavier hypernuclei can help answer this question. Indeed, the relevance of the mean-field approximation in nuclear physics is one of the prime questions related to role that the sub-structure of nucleons plays in the nucleus. It was, for example, suggested that the mass dependence of the binding energy difference between s and d orbitals may provide information on the "distinguishability" of a Λ hyperon as a baryon in nuclear medium [7].

The effective Λ-Nucleus interaction can be derived from a Λ-nucleon interaction such as the YNG or Njimegen potential forms [8]. The Njimegen potentials are obtained from phenomenological OBE fits to the baryon-baryon data using SU(3) with broken symmetry. The fit well represents the N-N and limited Y-N data. The YNG analytical form of the Λ-N effective interaction [9] is particularly useful in calculating hypernuclear binding energies, level structure, and reaction cross sections and polarizations. Because the Y-N interactions are weaker than N-N, and the Pauli exclusion principle is absent for the Λ hyperons in nucleus, hypernuclear properties can be reliably calculated. Therefore, experimental observables can be connected in

a straightforward way to YN interactions, and precision spectroscopic data can constrain the elementary Λ-N interaction. Indeed, because hyperon-nucleon scattering data cannot be easily obtained, the interaction is mainly constrained by hypernuclear structure.

1.2 Recent hypernuclear investigation

Although the spectra of many light Λ hypernuclei have been studied, there are only a few experiments on hypernuclear systems beyond the *p*-shell. Most of these later data were obtained using the (π^+, K^+) reaction, which strongly populates deeply-bound, high-spin states due to the large momentum transfer in this reaction. The BNL-AGS experiments surveyed the single particle nature of Λ hypernuclei up to ${}^{89}_{\Lambda}\mathrm{Y}$, and observed peaks corresponding to the major Λ shell structure [1]. The KEK E140a experiment made an intensive spectroscopic study using the SKS spectrometer, and observed the major shell structure of the single particle Λ orbits up to ${}^{208}_{\Lambda}\mathrm{Pb}$ [2, 10]. These spectra, shown in Fig. 1 were interpreted in terms of a Λ bound in a Woods-Saxon, density-dependent potential. However, the spectra are of poor quality as seen in the spectra, and the peak positions of the various shell structures were not well determined. Resolutions varied from 1.5 to 4 MeV FWHM from the light to heavy systems.

The best hypernuclear spectrum in the medium-heavy mass region was taken for the ${}^{89}_{\Lambda}\mathrm{Y}$ by the (π^+, K^+) reaction having an energy resolution of 1.7 MeV (FWHM). This spectrum is shown in Fig. 2 [11]. In addition to the major shell structure, the figure clearly shows the splitting of the higher shell orbitals, e.g. the *f* orbit. The origin of this splitting is under intensive discussion, and may be related to the hypernuclear *ls* splitting.

The progress (π^+, K^+) reaction spectroscopy has largely been driven by the superconducting kaon spectrometer (SKS), which has momentum resolution of 0.1 %, and a large solid angle of 100 msr [12, 13]. Using this spectrometer as a microscope, an intensive spectroscopic study of Λ hypernuclei has been undertaken at KEK. Binding energies of a Λ within nuclei as heavy as Pb have been extracted from the spectra, and the central part of the Λ hyperon potential has been experimentally investigated .

For *p*-shell Λ hypernuclei, high quality hypernuclear spectra have been derived again by the (π^+, K^+) reaction at KEK PS and the structure information on light Λ hypernuclei were obtained [3]. The spectra yielded information on the hypernuclear structure such as core excited states and also on spin-dependent ΛN interaction. A sample spectrum for the ${}^{12}\mathrm{C}(\pi^+,\mathrm{K}^+)$ reaction is shown in Fig. 3.

Other recent progress in hypernuclear spectroscopy involves the observation of γ transitions between hypernuclear states which are excited by pion or kaon production reactions. The γ rays are observed by Germanium and NaI detectors in coincidence with the production of bound hypernuclear levels. Because the splitting of the hypernuclear states by spin-dependent interactions (spin-spin and spin-orbit) is small, high precision γ ray spectroscopy is the only technique available which can directly measure these splittings. Of course identifying hypernuclear as opposed to nuclear gammas is difficulty and is presently limited to states in light Λ hypernuclei in the low excitation region. Previously observation of the ${}^{7}_{\Lambda}\mathrm{Li}$ E2 and M1 transition gave crucial information on the spin-spin interaction, and the structure change of the nucleus when a Λ is added to the system [15]. The observation of the E1 gamma

transition between the $p_{3/2}$ excited and the $s_{1/2}$ ground states of $^{13}_{\Lambda}$C [17] and the determination of the splitting between $5/2^+$ and $3/2^+$ spin-orbit partners in $^{9}_{\Lambda}$Be [16] confirmed the smallness of the ΛN spin-orbit splitting.

Both reaction and the γ ray spectroscopy have greatly advanced in the past few years, but spin splittings are too small to be observed by reaction spectroscopy. The best energy resolution achievable by the (π^+, K^+) reaction spectroscopy is 1.5 MeV (FWHM), and is mainly dependent on beam quality and target thickness. Thus until improved kaon and pion beams of much higher intensity become available, this resolution cannot be improved.

In summary, the present issues in hypernuclear spectroscopy are as follows.

- One would like to know the extent to which the single-particle properties of a baryon remain unchanged in deeply bound states. This can be explored by placing a Λ hyperon deeply within the nucleus.
- One would like to determination the spin dependent interaction strengths, of the effective Λ-Nucleus and thus extract the form of the Λ-N potential.

Although the spin-dependent interaction is best intensively studied in the *p*-shell by the γ-ray spectroscopy, complementary information from higher mass nuclei and higher excitation energies will be important. However the single particle nature of the Λ hyperon embedded in nuclear matter must be studied by the spectroscopy of heavy hypernuclei, and this is the key motivation of this proposal.

1.3 Experimental objectives

The proposed experiment is intended to establish high-precision spectroscopy of Λ hypernuclei for wide mass range by the (e,e'K^+) reaction. Such experimental investigation is possible only by utilizing the high precision and power of the Jlab electron beam, and a new high resolution, large solid-angle spectrometer system under construction.

The experimental objectives of the proposal are summarized below.

1. We propose to obtain high-precision binding energies of Λ single particle states from the excitation spectra of Λ hypernuclei up to A=50 region.

   The limited resolution of the (π^+, K^+) reaction makes it difficult to extract precise Λ binding energies, except for the light Λ hypernuclei. Energy resolutions of a few 100 keV are needed to extract these binding energies. This information provides the depth of the central potential and possible spin-orbit splittings over a wide mass region. The mass dependence of the single particle levels can be directly compared to calculations using single particle potentials and mean-field theory. Since *p*-shell orbitals are barely bound in *p*-shell hypernuclei, it is essential to extend this measurement to heavier systems. The proposed experiment also provides information on the widths of these single particle orbitals.

   As the effective mass of a Λ hyperon appears to be close to that of the free Λ hyperon, the potential seems to be local in contrast to ordinary nuclei. Thus the proposed precision measurement of the single particle levels can address the degree of non-locality of the effective Λ-Nucleus potential. This can be related

to the nature of the ΛN and ΛNN interactions, and to the ΛN short range interactions [18].

In a more exotic way, the binding energies can be discussed in terms of the distinguishability of a Λ hyperon in nuclear medium, which will result in different A dependence of the binding energy as suggested by Dover [7].

2. We propose to study the spin-orbit splitting of the Λ single particle states in heavier hypernuclei. As previously discussed, the ^{89}Y spectra taken by the (π^+, K^+) reaction show that the higher l states are split by about 1 MeV. These splittings are suggested to be due to the ΛN ls interaction, although the magnitude of the splitting is much larger than expected from previous measurements in the p-shell, and in particular from the recent γ ray data of $^{9}_{\Lambda}$Be and $^{13}_{\Lambda}$C [16, 17]. However the splitting could also be due to an interplay of different neutron hole states. With a resolution of about 300 keV, we will be able to entangle closely degenerate hypernuclear states, and clarify the situation. If the origin of the splitting is due to ls interaction it will give us the magnitude of the interaction, and introduce a deeper puzzle about the changes in the ls strength between the p and deeper shell structure. If the splitting is due to hypernuclear structure, it will give us information on the characteristics of medium-heavy hypernuclei. In either case, new information is required to address this issue.

3. We propose to study the ^{12}C(e,e'K$^+$)$^{12}_{\Lambda}$B reaction as a reference reaction in order to tune the new spectrometer system. As a byproduct of this calibration we will accumulate a high statistics $^{12}_{\Lambda}$B spectrum with a resolution of a few 100 keV. This should clearly separate the controversial core excited states. These states were observed in the ^{12}C(π^+,K$^+$) reaction, and a high precision - high statistics study will provide information on inter-shell mixing and perhaps on the splitting of the ground state doublet [14, 24, 25].

2 The (e,e'K$^+$) reaction for the hypernuclear spectroscopy

2.1 Hypernuclear production reactions

The (e,e'K$^+$) reaction has a unique characteristics for the hypernuclear spectroscopy among a wide variety of reactions which can be used to produce a strangeness -1 hyperon as listed in Table 1. Each reaction has its own characteristics and will plays its role for hypernuclear spectroscopy. However, only the (K^-, π^-) and (π^+, K^+) reactions have been intensively used for the spectroscopic investigation in these reactions, so far. These reactions supposed to convert a neutron in the target nucleus to a Λ hyperon. Although the (π^+, K^+) reaction is relatively new compared to the (K^-, π^-) reaction, it is now considered as one of the best reactions for hypernuclear spectroscopy because it favorably populates deeply bound hypernuclear states [1, 14, 2]. The smaller cross sections of the (π^+,K$^+$) reaction compared to that of the (K$^-$,π^-) reaction is easily compensated by intensity of pion beams, which is much higher than that of kaon beams. The (π^+,K$^+$) reaction selectively populates angular momentum stretched states because of the large momentum transfer to the recoil hypernuclei [19, 20, 18]. This is in contrast to the (K^-, π^-) reaction, which transfers small momentum and thus preferentially excites

Table 1: Comparison of Λ Hypernuclear production reactions

$\Delta Z = 0$ *neutron to* Λ	ΔZ = -1 *proton to* Λ	comment
(π^+, K^+)	(π^-, K^0)	stretched,high spin
in-flight (K^-, π^-) stopped (K^-, π^-)	in-flight (K^-, π^0) stopped (K^-, π^0)	substitutional
$(e, e'K^0)$ (γ, K^0)	$(e, e'K^+)$ (γ, K^+)	spin-flip,unnatural parity

substitutional states. By high quality (π^+, K^+) spectra with resolution better than 2 MeV (FWHM), it becomes possible to qualitatively study the unique structure of Λ hypernuclei and characteristics of the Λ-nucleon interaction.

2.2 The (e,e'K$^+$) reaction

Since the momentum transfer of the (e,e'K$^+$) reaction is almost the same as that of the (π^+, K^+) reaction, it is expected to preferentially populate high-spin bound hypernuclear states. However, in contrast to reactions with meson beams, the electromagnetic reaction will populate spin-flip hypernuclear states as well as non-spin-flip states, since the transition operator has spin-independent (f) and spin-dependent (g) terms [21, 22]. Although the spin independent term is significantly smaller than the spin-dependent term, the spin-flip and non-spin-flip components in the spin-dependent term have comparable amplitudes.

Also the (e,e'K$^+$), in contrast to the (π^+, K^+) and (K^-, π^-) reactions, converts a proton to a Λ hyperon. This results in proton-hole-Λ-particle states in the configuration $[(lj)_N^{-1}(lk)^\Lambda]_J$. When the proton hole state is $j_> = l + 1/2$, the highest spin states of $J = J_{max} = j_> + j_>^\Lambda = l_N + l_\Lambda + 1$ are favorably excited. These hypernuclear states are of unnatural parity when the original proton orbit is $J_>$. On the other hand, if the hole state has spin $j = j_< = l - 1/2$, the highest spin states of the multiplet $J'_{max} = j_< + j_>^\Lambda = l_N + l_\Lambda$ with natural parity are strongly populated. This selectivity is particularly important as it allows us to directly study the spin-dependent structure of Λ hypernuclei.

Experimentally, the most important characteristics of the (e,e'K$^+$) reaction is that it can provide significantly better energy resolution because the reaction is initiated with a primary electron beam of extremely good beam emittance, in contrast to secondary meson beams. With a high performance spectrometer, energy resolution of a few 100 keV can be achieved.

The unique characteristics of the (e,e'K$^+$) reaction are summarized below.

- Extremely good energy resolution when coupled with the high resolution kaon spectrometer (HKS) under construction in Japan.
- The production of natural and non-natural parity states.

- The production of neutron rich hypernuclei as the reaction replaces a proton by a Λ.
- calibration of the (e,e'K^+) reaction can be performed by the elementary p(e,e'K^+)Λ reaction on a CH_2 target which provides an exact energy scale.

Although the (e,e'K^+) reaction has many advantages for hypernuclear spectroscopy, it has disadvantage that the cross section is much smaller than reactions using hadronic beams. For example, the calculated cross section for the ^{12}C(e,e'K^+)$^{12}_{\Lambda}$B$_{gr}$ is two orders of magnitude smaller than that of the corresponding ^{12}C(π^+,K^+)$^{12}_{\Lambda}$C$_{gr}$ reaction. With the E89-009 setup, hypernuclear yields of the ground state of $^{12}_{\Lambda}$B are smaller by almost two order of magnitude compared with that of $^{12}_{\Lambda}$C by the SKS experiment. However, this disadvantage can be overcome by employing a new geometry which we propose for this experiment. The new geometry uses a new Kaon spectrometer, HKS, which is described in the next section.

2.3 Previous E89-009 experiment

The first hypernuclear electro-production experiment has been successfully completed in Hall C at Jlab in the spring of 2000. This experiment used the ^{12}C(e,e'K^+)$^{12}_{\Lambda}$B reaction, and observed the ground state peak of $^{12}_{\Lambda}$B hypernucleus. The experiment demonstrated that Λ hypernuclear spectroscopy can be performed by the (e,e'K^+) reaction and that sub-MeV energy resolution can be obtained as shown in Fig. 4. The resolution obtained in the experiment, $\sim$ 650 keV, is better by a factor of 3 than that previously obtained.

The E89-009 experiment was designed to take advantage of the peak in the virtual photon flux at very forward angles. Thus it had low luminosity since a maximum number of photons/incident electron were available for reactions. The experimental setup is schematically shown in Fig. 5. Zero degree electrons and positive kaons were bent into their respective spectrometers on opposite sides of the beam by a splitter magnet. The electron momentum was analyzed by a small Split-Pole spectrometer positioned to detect zero degree electrons. Positive kaons were detected also at around 0 degrees using the SOS spectrometer. Typical count rates of each particle in the Enge and SOS spectrometers were summarized in section 14.4 of Appendix B. The experiment utilized a low beam current of 0.66 μA with a ^{12}C target 20 mg/cm^2 thick.

Although the experiment was successful, the yields were limited due to the background flux of bremsstrahlung in the electron spectrometer. We had recognized that further improvement of experimental configuration would be required to extend these studies to heavier systems. However E89-009 was needed to provide valuable information on rates and cross sections in order to design a geometry which could be successfully be extended.

3 Proposed experiment

3.1 Experimental goals

Based on the experience obtained in the E89-009 experiment, we plan to take into account the following two key points for the proposed experimental configuration.

- A new high resolution kaon spectrometer (HKS) which is under construction will have 20 msr solid angle with the splitter and simultaneously achieve around a few 100 keV resolution.
- A new experimental configuration will maximize hypernuclear production rates by avoiding the 0-degree bremsstrahlung electrons but still measure scattered electrons at a sufficiently forward angle. "Tilt method" in which the Enge electron spectrometer is tilted by 2-3 degrees vertically will allow us to accept a beam current as high as a few tens μA.

It is emphasized that hypernuclear yield/nb/sr is approximately inversely proportional to hypernuclear mass number with the proposed "Tilt method", while the beam intensity was limited by brems electron rates since it is governed by inverse of $Z^{2+\delta}$ when the 0 degree tagging method is employed. Therefore, the "Tilt method" is much advantageous for the spectroscopy of heavier Λ hypernuclei than the "0 degree tagging method". The new "Tilt method" inherits advantageous aspects of the 0-degree tagging method, but allows us to accept much higher beam currents because the high rate brems electrons are not allowed to enter the Enge spectrometer.

3.2 Proposed experimental condition

In the proposed experiment, the followings were taken into account to optimize experimental conditions for high-resolution and high efficiency hypernuclear spectroscopy.

1. As shown in Fig. 6 and Fig. 7, angular distributions of virtual photons and kaons in the (e,e'K^+) reaction is forward peaked and thus both the electron and the kaon spectrometer should be positioned at as forward angles as possible.
2. The virtual photons at 0 degrees have the energy, E_γ, is given as,

$$E_\gamma = E_e - E_{e'} \tag{1}$$

   where E_e and $E_{e'}$ are beam and scattered electron energies. The elementary cross section of the (γ,K^+) reaction has relatively weak E_γ dependence above the threshold.
3. Once the energy of virtual photon is fixed, outcoming K^+ momentum is given assuming hypernuclear mass. P_{K^+} is about 1 GeV/c for E_γ = 1.8 - 0.3 = 1.5 GeV where the scattered electron energy is assumed to be 0.3 GeV as an example. Photon energy effective for the production of kaons will have a range that corresponds to the energy acceptance of the electron spectrometer. Thus, the momentum acceptance of the kaon spectrometer and the electron spectrometer should match each other.
4. Maximum kaon momentum to be detected should be optimized considering
   (a) Yield of hypernuclei
   (b) Energy resolution and acceptance of the spectrometer. Naturally, the energy resolution becomes worse with higher momentum.
   (c) Particle identification, particularly between pions and kaons.

(d) Size of the kaon spectrometer and consequently construction cost.

5. For the yield of Λ hypernuclei, three factors contribute,

   (a) The elementary cross section of $p(\gamma,K^+)\Lambda$ is almost constant for the energy range of real γ from 1.1 - 2.0 GeV. Corresponding kaon momentum is from $\sim$ 0.7-1.6 GeV/c. However, the hypernuclear cross sections get greater with the higher γ energy because the recoil momentum becomes smaller.

   (b) With higher kaon momentum, the survival rate of the kaon becomes higher for the given flight path of the spectrometer.

   (c) With higher kaon momentum, the cone of scattered kaons becomes narrower. Thus, larger fraction of the hypernuclei produced in the reaction will be captured for the same solid angle if the spectrometer is positioned at or close to 0 degrees.

   The figure of merit as a function of electron energy assuming the scattered electron energy is 0.285 GeV is shown in Fig. 8. It is shown the higher the energy of the electron beam, the larger the yield of the hypernuclear ground states for a given spectrometer configuration.

6. Although the hypernuclear yield is expected to increase with beam energy, reaction channels strangeness production other than a Λ hyperon open at higher energy and will become sources of background, because that bremsstrahlung photons up to the beam energy are produced in the targets. The electron beam energy is better kept as low as possible from the points of background and particle identification.

7. Taking into account above conditions, the optimum kaon momentum is set at 1.2 GeV/c aiming 2×10^{-4} momentum resolution. The momentum resolution corresponds to about 100 keV energy resolution in hypernuclear excitation spectra.

8. The electron spectrometer also should have momentum resolution of $\leq 3 \times 10^{-4}$, matching that of the kaon spectrometer. Since the momentum of scattered electron is low compared to that of kaons, better momentum resolution can be achieved.

3.3 Proposed experimental geometry

The E89-009 experimental setup accepted reaction electrons and kaons at angles down to zero degrees. The singles rates in each arm of electrons, positrons, pions and protons were analyzed and compared with theoretical calculations. However the calculated rates were renormalized to the experimental rates when used for the various estimates to be described below. It was found that the 0-degree electron-tagging method was limited by the accidental rate from bremsstrahlung electrons. We therefore propose to tilt the electron spectrometer by a small angle sufficient to exclude electrons from the bremsstrahlung process. This technique is described in detail in Appendix A.

A plan view of the proposed geometry, splitter+Enge spectrometer +high resolution kaon spectrometer (HKS), is shown in Fig. 9. Both the HKS spectrometer and the Enge spectrometer are positioned as far forward in angle as possible,

without accepting 0-degree electrons or positrons. The HKS spectrometer, having a QQD configuration, was designed for the kaon arm. Details are found in the Appendix B. It has a momentum resolution of 2×10^{-4} at 1.2 GeV/c, and a large solid angle of 20 msr, including the splitter. This is summarized in Table 2.

In designing the proposed experiment, data taken in E89-009 experiment were analyzed and singles rates of electrons, positrons, pions and protons in each arm were extracted. These are compared with the EPC code calculations and the normalization factors were derived. Assuming the obtained normalization factor for the hadron production rate at the forward angles, singles rates of the counters in the proposed setup were evaluated.

For the scattered electrons, the Enge split-pole spectrometer used for the E89-009 experiment will be adopted. However, the spectrometer is to be vertically tilted by 2.25 degrees so that the Bremsstrahlung electrons will not enter the spectrometer acceptance. The components of the focal plane detector system are redesigned and are explained later.

The splitter magnet has the same geometry used in E89-009 but the gap will be widened so that it matches the HKS geometrical acceptance.

The configuration and specification of the proposed hypernuclear spectrometer system is summarized in Table 2 and is shown in Fig. 9.

Table 2: Experimental condition and specification of the proposed hypernuclear spectrometer system

Beam condition	
Beam energy	1.8 GeV
Beam momentum stability	1×10^{-4}
General configuration	Splitter+Kaon spectrometer+Enge spectrometer
Kaon spectrometer	
Configuration	QQD and horizontal bend
Central momentum	1.2 GeV/c
Momentum acceptance	$\pm$ 10 %
Momentum resolution ($\Delta p/p$)	2×10^{-4}
	(beam spot size 0.1mm assumed)
Solid angle	20 msr with a splitter
	(30 msr without splitter)
Kaon detection angle	Horizontal : 7 degrees
Enge split-pole spectrometer	
Central momentum	0.3 GeV/c
Momentum acceptance	$\pm$ 20 %
Momentum resolution ($\delta p/p$)	2×10^{-4}
Electron detection angle	Horizontal : 0 degrees
	Vertical : 2.25 degrees

3.4 Proposed reactions

1. **p(e,eK$^+$)Λ reaction**

   The reaction is used to calibrate the spectrometer system with a CH_2 target for

the absolute missing mass scale. The procedure has been established in the E89-009 experiment. By the known Λ mass, the absolute scale of the binding energy can be determined reliably. Since we aim to determine absolute binding energies of a Λ hyperon in the mass region where no emulsion experiments can be applied, the reaction is important for the present experiment. It is in contrast to the (π^+, K^+) reaction in which we have to rely on other in direct reactions since a neutron target is not available.

2. **^{12}C(e,e'K$^+$)$^{12}_{\Lambda}$B reaction**

   The reaction is used as a reference reaction for examining overall performance of the spectrometer. Since the excitation function of $^{12}_{\Lambda}$B is expected relatively simple and high statics data can be obtained in relatively short data taking hours, the reaction will allow us to optimize the optics of the entire system thus the overall missing mass resolution. Also, short runs before any beam period will allow us to correct any possible shifts in the system settings.

   In addition, the reaction will provide us with significant physics information. As already mentioned in the preceding section, the $^{12}_{\Lambda}$C hypernucleus studied by the (π^+, K^+) reaction revealed hypernuclear core excited states for the first time. Since then, the excitation energies of the 1^-_2 and 1^-_3 states which supposed to be generated by coupling of a Λ hyperon in the s orbital and the core excited ^{11}C have been under intensive discussion. Role of intershell mixing of positive-parity states and the relation with the ΛN spin-spin interaction have been suggested [24, 25]. Precision spectrum of the mirror symmetric Λ hypernucleus, $^{12}_{\Lambda}$B, with much better resolution will resolve these states unambiguously as demonstrated in Fig. 10 and the excitation energies and cross sections of the states will be determined reliably. We also intend to determine or set the limit of spin-spin splitting of the ground state since the (e,e'K$^+$) reaction populates both states in comparable strengths. Due to the high yield of the new geometry and statistics needed for calibration of system optics, the angular distributions are automatically measured for the major shell states because of the large HKS angular acceptance.

3. **^{28}Si(e,e'K$^+$)$^{28}_{\Lambda}$Al reaction**

   The ^{28}Si$(\pi^+$,K$^+)^{28}_{\Lambda}$Si reaction was studied using the SKS spectrometer, a spectrum of which is shown in Fig. 11 [2]. In the spectrum, major shell structure corresponding to the s and p orbitals with 2 MeV (FWHM) resolution was seen. At the same time unexpected peak structure was observed between the two peaks, although the origin is not known. Since the mass dependence of Λ spin-orbit splitting of the p orbital is expected to be almost maximum at $^{28}_{\Lambda}$Si, it was also aimed to resolve the splitting.

   The excitation spectrum of the ^{28}Si$(\gamma$,K$^+)^{28}_{\Lambda}$Al reaction has been calculated at $\mathrm{E}_\gamma = 1.30$ GeV and $\theta = 3$ degrees. A simulated spectrum assuming the spin-orbit strength ($\mathrm{V}_{so} = 2$ MeV) with 300 keV (FWHM) resolution and with expected statistics for the proposed running time is shown in Fig. 12. Peaks corresponding to each major shell orbitals will be distinctively identified and their binding energies will be derived reliably. For a Λ hyperon in the p orbital, $[\pi d^{-1}_{5/2} \otimes \Lambda p_{3/2}]4^-$ and $[\pi d^{-1}_{5/2} \otimes \Lambda p_{1/2}]3^-$ states are dominantly populated, providing a good opportunity to directly observe the ls splitting. Figure 12 clearly demonstrates possibility of observing the splitting.

4. **^{51}V(e,e'K$^+$)$^{51}_{\Lambda}$Ti reaction**

   In the ^{51}V target, the neutron $f_{7/2}$ shell is well closed and stable because N=28. The reaction is supposed to convert one of the three protons in the f-shell to a Λ hyperon. In this hypernuclear mass region, a hyperon is bound up to the d-orbital, providing us an opportunity to determine the binding energies up to higher l. The hypernucleus, $^{51}_{\Lambda}$V, was studied by the (π^+, K^+) reaction at BNL with resolution around 3 MeV (FWHM) and it is shown in Fig.13 [1]. The quality of the spectrum is poor but the major shell structure is seen. For the (γ,K^+) reaction, a model calculation has been carried out similarly as ^{28}Si$(\gamma,\mathrm{K}^+)^{28}_{\Lambda}$Al [26, 22]. In Fig.14, the calculated excitation spectrum is shown. The $[\pi f_{7/2}^{-1} \otimes \Lambda d_{5/2}]6^-$ and $[\pi f_{7/2}^{-1} \otimes \Lambda d_{3/2}]5^-$ states, which are spin-orbit partners, are expected to be split by more than 1 MeV if $V_{so} = 2$ MeV. The calculated spectrum suggests that these states will be simultaneously populated and can be observed in the (e,e'K$^+$) reaction.

   Since nuclei in this mass region are rather well described by shell-model wave functions, it is expected that comparison between experimental data and theoretical calculations will have less ambiguities. We will therefore have a good chance to investigate the single-particle nature of a Λ hyperon and also investigate the splitting of the single particle states not only in the s and p orbitals but also in the d orbital.

5. **^{89}Y(e,e'K$^+$)$^{89}_{\Lambda}$Sr reaction**

   As mentioned already, $^{89}_{\Lambda}$Y is the Λ hypernucleus studied with the best statistics in medium-heavy mass region by the (π^+, K^+) reaction. As seen in Fig. 2, in addition to the major shell peak structure, splitting of these peaks were observed. If the (e,e'K$^+$) reaction can be applied to this heavier mass region, we will better investigate Λ hyperon single-particle nature and also splitting of these states by ΛN interaction. Therefore, we also propose to conduct an exploratory R&D run with the ^{89}Y target to examine feasibility of extending the (e,e'K$^+$) hypernuclear spectroscopy to the heavier mass region.

4 Experimental setup and expected performance

In this section, we describe the proposed experimental setup and also the expected performance of the spectrometer system which is evaluated based on the experience of E89-009. Further detail of the HKS spectrometer design and construction plan will be given in Appendix B.

4.1 General configuration

The present spectrometer system consists of 1) the HKS spectrometer for the kaons, 2) Enge spectrometer for the scattered electron and 3) the splitter. In Fig. 15, plan view of the spectrometer system installed in Hall C is shown. It would fit in the space between the HMS-SOS pivot and the G0 detector system. Our intention is to install the spectrometer system as upstream us possible so that the interference with the G0 experimental setup is minimum. It is required that the beam swingers are installed downstream of the splitter magnet and the beam is directed to the beam dump of Hall C. It is necessary since the high intensity beam of 30 μA are required

in the proposed experiment, contrasting E89-009 which used low beam current of about 1 μA.

4.2 High resolution Kaon spectrometer (HKS)

General specifications of the HKS spectrometer are given in Table. 2. The HKS is designed to achieve simultaneously 2×10^{-4} momentum resolution and 20 msr solid angle acceptance with the splitter. Figure 16 shows the angular and momentum acceptance of the HKS spectrometer with the splitter calculated with a GEANT simulation code. The HKS is placed rotated horizontally by 7 degrees with respect to the beam to avoid zero degree positive particles, mostly positrons. The solid angle is more than 20 msr over the momentum region of 1.2 GeV/c $\pm$ 10%, as designed. Figure 17 shows the momentum resolution obtained with the code as a function of momentum for three different positions of the tracking chambers with respect to the focal plane. In the simulation, realistic matter distributions such as a vacuum window and chamber windows, and drift chamber position resolutions were taken into account. Even with a modest chamber resolution of 200 μm, momentum resolution of 2×10^{-4} will be achieved.

The detector system for the HKS and Enge is summarized in Table 3. The HKS detector system has similar configuration to the one in SOS. However, as seen in Table 4, HKS singles rate is dominated by pions, whose rate will be up to a few MHz. In order to achieve efficient pion rejection rate as high as 10^{-4}, two layers of aerogel Cerenkov counter with refractive index of 1.055 will be installed. For the proton rejection, Lucite Cerenkov counter with wavelength shifter in it will be employed, so that the Cerenkov counter has good efficiency for the wide range of incident angles. Time resolution of as good as 80 ps is a goal for the time-of-flight scintillators. By having the good time resolution, we plan to minimize the distance between the two time-of-flight wall and achieve large solid angle. A Gas Cerenkov counter will also be installed as a trigger counter so that positrons can be tagged for calibration purposes. The tracking chambers of HKS should have high rate capability and accept the rate up to a few MHz.

4.3 Enge spectrometer

The Enge spectrometer which was used in E89-009 will be installed as a spectrometer to analyzes scattered electron momentum. However, as already mentioned, the spectrometer will be tilted vertically by 2.25 degrees, which was not the case in the previous E89-009 experiment.

The detectors required at the Enge are also summarized in Table 3. For the Enge spectrometer, tracking of the electrons are required to achieve good momentum resolution since it is tilted and the focal plane is no more the one originally designed. The expected rate is only a few MHz and is 2 order of magnitude smaller than the case of E89-009, in which the beam intensity as limited by this Brems electron rate.

The optics of the combined system of Splitter plus the tilted Enge spectrometer shows the same general features about focal plane geometry and momentum dispersion as the original untilted geometry used in E89-009. However, with the introduced tilted angle with respect to the horizontal plane, the momentum correlates to all the focal plane parameters, x, x', y, and y', where the x' and y' are the in-plane and out-of-plane angles, respectively. Thus, a full tracking including

both position and angular measurements is needed. The momentum resolution is studied as a function of position and angular errors as shown in Fig.18. The dominant contributions are from x and x', which means that the measurements in y and y' are less crucial. The results showed that using a 4th-order optical matrix and the momentum resolution can be better than 3×10^{-4} (FWHM), if the position error is about 0.15 mm (r.m.s.) and the angular error is about 1 mr (RMS). Such precision can be easily reached by the conventional wire chamber technique and the multiple scattering contributions from the light vacuum window material used in the HNSS experiment and wire chambers is small, if the first tracking plane is located along the focal plane. With a central momentum about 300 MeV/c, the resolution contribution is about 90 keV (FWHM) or less, thus small compare to other contributions. Similarly segmented scintillation hodoscope array as used in the HNSS experiment will be used. The thickness will be increased to improve the time resolution of 250 ps achieved in the HNSS experiment for better signal /accidental separation. An on-line coincidence between the e' and K^+ will be used for this proposed experiment to reduce the data size.

Table 3: Detectors for the proposed experiment

Nomenclature	Size	Comments
HKS spectrometer		
Drift chamber		
HDC1	$30^H \times 90^W \times 2^T cm$	xx'uu'(+30deg)vv'(-30 deg) 5 mm drift distance
HDC2	$30^H \times 105^W \times 2^T cm$	xx'uu'(+30deg)vv'(-30 deg) 5 mm drift distance
Time of flight wall		
TOF1	$30^H \times 110^W \times 2^T cm$	7.5^W cm × 15-segments, H1949
TOF2X	$30^H \times 130^W \times 2^T cm$	7.5^W cm × 17-segments, H1949
TOF2Y	$30^H \times 130^W \times 1^T cm$	4^W cm × 8-segments, H1161
Cerenkov counter		
AC1	$40^H \times 135^W \times 30^T cm$	n = 1.055 water-proof aerogel 16 × 5" PMT
AC2	$40^H \times 135^W \times 30^T cm$	n = 1.055 water-proof aerogel 16 × 5" PMT
LC	$40^H \times 135^W \times 2^T cm$	7.5^W cm × 18-segments, H1161 Lucite with wavelength shifter
GC	$40^H \times 200^W \times 100^T cm$	10 × 5" PMT
Enge spectrometer		
Drift chamber		
EDC1	$10^H \times 72^W \times 10^T cm$	VDC
EDC2	$10^H \times 72^W \times 10^T cm$	VDC
Hodoscope		
EHODO	$10^H \times 80^W \times 1^T cm$	80 segmentation

4.4 Singles rates

Count rates in HKS and Enge spectrometers were estimated as follows:

1. π^+ and proton rates in HKS were calculated based on the EPC code, and were normalized by the experimental values measured in E89-009 for a carbon target at 2.2 degrees. The data obtained in E89-009 are summarized in section 14.4 of Appendix B.
2. Quasifree kaon production cross section was assumed to scale as $A^{0.8}$.
3. Electron rate in Enge was evaluated by two methods, one by EGS code and the other by Light body code, which agreed more or less to each other.
4. Pion rate in Enge was calculated based on the EPC code, and normalized by the same factor used for hadron rates in HKS.

As seen in Table 4, singles rate of HKS is dominated by positive pions. while that for Enge is by electrons. It is noted that we expect the positron rate in HKS is low since we setup HKS at an angle off 0 degrees. The singles rate of the ENGE hodoscope is expected almost two orders of magnitude less than that of E89-009. With this rate, the hardware coincidence between electron arm and kaon arm can form good triggers.

Table 4: Singles rates

Target	Beam Intensity (μA)	HKS e^+ rate (MHz)	HKS π^+ rate (kHz)	HKS K^+ rate (Hz)	HKS p rate (kHz)	Enge e^- rate (MHz)	Enge π^- rate (kHz)
^{12}C	30	-	800	340	280	2.6	2.8
^{28}Si	30	-	800	290	240	2.6	2.8
^{51}V	30	-	770	260	230	2.6	3.0

4.5 Resolution of excitation energy spectra

The following factors contribute to the total resolution of the experiment:

1. HKS momentum resolution
   With a Monte Carlo simulation, the momentum resolution of the HKS was estimated to be 75 keV/c (RMS) for a spatial resolution of 200μm of the chambers.
2. Beam momentum resolution
   Assuming 1×10^{-4}, it will be 180 keV/c (FWHM) for 1.8 GeV/c beam.
3. Enge momentum resolution
   For vertical and horizontal resolutions of the chamber as 150μm, the momentum resolution of the Enge spectrometer is estimated to be 93 keV (FWHM).
4. Kinematical broadening due to uncertainty of the K^+ scattering angle
   The uncertainty of the K^+ emission angle is dominated by the multiple scattering through the materials between the target and the chambers

(uncertainty due to the spatial resolution of the chambers are less than 0.2 mrad). Contribution of the following materials are taken into account: the target (100 mg/cm^2), vacuum windows (kevlar 0.008", mylar 0.005"), helium bag (100 cm) and chambers (mylar 0.0045", argon 5.08 cm @ STP).

Total uncertainty of the K^+ angle was estimated to be 3.3 mrad (r.m.s.) for the carbon target. This angular uncertainty corresponds to 152 keV (FWHM) ambiguity to the $^{12}_{\Lambda}$B mass. Similarly, this effect to $^{28}_{\Lambda}$Al (Si target) will be 64 keV (FWHM).

5. Momentum loss in the target
The momentum loss in the target was calculated for 1.2 GeV/c K^+ assuming Vavilov distribution. The whole momentum loss in the target will contribute the mass resolution without any correction. The average momentum loss of 1.2 GeV/c K^+ in the carbon 100 mg/cm^2 was 195 keV/c which corresponds to the energy resolution of 180 keV(FWHM).

The results are summarized in Table 5. Present proposed experimental setup will achieve the resolution around 300 keV (FWHM).

Table 5: The energy resolution of the HKS system

Item	Contribution to the resolution (keV, FWHM)			
Target	C	Si	V	Y
HKS momentum			190	
Beam momentum			$\leq$ 180	
Enge momentum			93	
K^+ angle	152	64	36	20
Target (100 mg/cm^2)	$\leq$ 180	$\leq$ 171	$\leq$ 148	$\leq$ 138
Overall	$\leq$ **360**	$\leq$ **330**	$\leq$ **320**	$\leq$ **310**

4.6 Background and signal/noise ratios

One of the major sources of background in the proposed setting that facilitates detection of very forward particles is electrons associated with Bremsstrahlung process. During the E89-009 experiment, a data was taken with Pb sheet blocking 0 degree Brems electrons just at the entrance of the Enge spectrometer. Although it was tricky to place a thin material at 0 degrees, it was learned that blocking 0 degree Brems electrons helps improve signal to noise ratio considerably by this 0-degree blocking technique. The Tilt method, which offers us 2 order of magnitude more hypernuclear yield and a factor of 10 better signal to noise ratio compared to the E89-009 setup.

Electron and positron rates were estimated as given in Table 4 for the beam current of 30 μA and the target thickness of 100 mg/cm^2. It shows that 2.6 MHz of the electron background in the Enge spectrometer which placed with 2.25 degrees to the beam axis (electron beam, 100 mg/cm^2 carbon target). Kaon single rate for the HKS spectrometer was estimated to be 340 Hz as shown in Table 4. With a coincidence window of 2 ns, we have accidental coincidence rate as:

$$N_{ACC} = (2.6 \times 10^6 \text{Hz}) \cdot (2 \times 10^{-9} \text{sec}) \cdot (340 \text{Hz}) \sim 1.8/\text{sec}.$$

Assuming that the accidental coincidence events spread uniformly over the energy matrix (Enge 149 MeV × HKS 240 MeV), the largest background per bin (100 keV) projected on the hypernuclear mass spectrum will be 8×10^{-4} /sec. A typical hypernuclear (^{12}C target) event rate will be 48.4 / (100 nb/Sr) / h = 1.3 $\times 10^{-2}$ / (100 nb/Sr) / sec as shown in Table 6.

Table 6: Expected hypernuclear production rates in the (e,e'K$^+$) reaction

Target	beam Intensity (μA)	Counts per 100nb/sr · hour	Qfree K$^+$ in HKS(Hz)
^{12}**C**	30	48.4	340
^{28}**Si**	30	20.7	288
^{51}**V**	30	11.4	228

5 Yield estimate and requested beam time

The expected yield of the hypernuclear states are evaluated based on the E89-009 result for $^{12}_{\Lambda}$B ground state in the ^{12}C(e,e'K$^+$)$^{12}_{\Lambda}$B reaction. As described in Appendix B, the proposed "Tilt method" is expected to realize more than factor of 50 yield gain. It is partly because we can use higher intensity beams and thick targets and partly because the kaon spectrometer has a larger solid angle acceptance.

The cross sections of the hypernuclear states for the targets, ^{12}C,^{28}Si,^{51}V have been calculated by Motoba and Sotona [26, 22]. They are listed in Table 7.

It is noted, however, the calculated cross sections vary by a factor of 2-5 depending on the choice of model parameters for the elementary reaction, hypernuclear potentials and configuration of the states etc. In the present yield estimate, the cross sections were normalized assuming the cross section of the ^{12}C(e,e'K$^+$)$^{12}_{\Lambda}$B reaction for the ground state doublet is 100 nb/sr.

For the beam time, we request commissioning beam time for the HKS itself as the spectrometer is newly installed. The performance of the HKS spectrometer, particularly momentum resolution, will be examined using the requested beam time for the commissioning.

It is our request that the commissioning beam time is allocated a few months before the tuning and data taking beam time so that we can analyze the data and understand the performance of the spectrometer in advance.

Tuning the spectrometer system coupled with the tilted Enge spectrometer will be carried out with a CH_2 target using the Λ peak and with the ^{12}C target.

The requested data taking hours for C, Si and V targets were calculated so that 3000 counts for ground states of $^{12}_{\Lambda}$B, 1000 counts for $^{28}_{\Lambda}$Al and 400 counts for $^{51}_{\Lambda}$Ti can be accumulated, assuming 50 % efficiency for data taking and data analysis. For $^{89}_{\Lambda}$Sr, the requested beam time is only for an exploratory run. The requested beam times are summarized in Table 8. Requested beam conditions are listed in Table 9.

Table 7: Cross sections of ${}^{12}_{\Lambda}$B, ${}^{28}_{\Lambda}$Al and ${}^{51}_{\Lambda}$Ti calculated by DWIA [26]

Target	Hypernucleus	Hypernuclear configuration	Cross section (nb/sr)
^{12}C	${}^{12}_{\Lambda}$B	$s_{1/2}$	112
		$p_{3/2}$	79
		$p_{1/2}$	45
^{28}Si	${}^{28}_{\Lambda}$Al	$s_{1/2}$	56
		$p_{3/2}$	95
		$p_{3/2}$	57
		$d_{5/2}$	131
		$d_{3/2}$	111
^{51}V	${}^{51}_{\Lambda}$Ti	$s_{1/2}$	18
		$p_{3/2}$	41
		$p_{3/2}$	26
		$d_{5/2}$	52
		$d_{3/2}$	48
		$1s_{1/2}$	16
		$f_{7/2}$	32
		$f_{5/2}$	38

6 Schedule of the spectrometer construction and requested support

The construction of the HKS spectrometer and the new hypernuclear spectrometer system has already started in 2000. The present schedule for the construction is shown in Table 10. It is the present plan to ship the HKS spectrometer system from Japan to Jlab by the end of 2002. Detectors are under construction by the collaboration groups and will also be prepared by then.

It is planned that the spectrometer system will be assembled in the Test Lab. prior to the installation in Hall C. The collaboration sets the due date ready to accept a beam March 2003.

7 Summary

High-resolution (e,e'K^+) spectroscopy for the four targets, ^{12}C, ^{28}Si, ^{51}V and ^{89}Y has been proposed. By the proposed spectroscopy, we plan to reveal 1) Single-particle nature of a Λ hyperon by deriving single particle binding energies and widths and/or splitting of the single-particle states in wide mass range; 2) Splitting of higher-l single particle states in view of ΛN ls interaction and also structural origin; and 3) Characteristic structure of ${}^{12}_{\Lambda}$B, ${}^{28}_{\Lambda}$Al, ${}^{51}_{\Lambda}$Ti and ${}^{89}_{\Lambda}$Sr. Puzzling core excited states in ${}^{12}_{\Lambda}$B(${}^{12}_{\Lambda}$C) will be intensively studied with high quality spectrum.

An exploratory spectrum will be also taken for the ^{89}Y target, in order to examine the possibility to extend hypernuclear spectroscopy to the heavier targets.

The present proposal assumes the high resolution kaon spectrometer (HKS) under construction by the Tohoku group with the Monbusho budget. The proposal

Table 8: Requested beam time

	Target	Hypernucleus	Number of days	Number of hours
HKS commissioning			7	168
Tuning and calibration			7	168
Data taking				
	^{12}C	$^{12}_{\Lambda}$B	4	96
	^{28}Si	$^{28}_{\Lambda}$Al	8	192
	^{51}V	$^{51}_{\Lambda}$Ti	14	336
	^{89}Y	$^{89}_{\Lambda}$Sr	4	96
Total			40	**960**

Table 9: Requested beam conditions

Typical beam energy	1.8 GeV
Typical beam current	30 μA
Beam energy stability	$\leq 1 \times 10^{-4}$

is fully based on the success of the E89-009 experiment carried out in the spring of 2000. Once the proposed experiment is successfully carried out, we envision that the hypernuclear physics program by the (e,e'K$^+$) reaction will be fully explored as 1) Λ hypernuclear spectroscopy for targets as heavy as Pb; 2) Intensive high quality spectroscopy of light Λ hypernuclei; and also 3) Open a path way toward weak decay experiments taking advantage of high-quality high-power electron beam at Jefferson Laboratory.

Table 10: Present expected time line of the project

April, 2000 - March, 2001	
	Design of the spectrometer system
	Contract with a magnet manufacture
	Construction of Q1 and Q1
	Design of detectors
April, 2001 - March, 2002	
	Construction of the dipole magnet
	R&D test of detectors (TOF, AC etc.)
	Design and construction of the drift chambers
	Design and construction of TOF, LC
April, 2002 - March, 2003	
	Field mapping of the dipole magnet
	Transportation of the dipole to Jlab
	Assembly and test of the spectrometer magnet at Jlab
	Completion of the detector construction
	Assembly of the detector system at Jlab
	Installation of the spectrometer system in the Hall

References

[1] C. Milner *et. al.*, Phys. Rev. Lett. **54** (1985) 1237;
P. H. Pile *et al.*, Phys.Rev.Lett.**66** (1991) 2585.

[2] T. Hasegawa *et al.*, Phys. Rev. **C53** (1996) 1210.

[3] O. Hashimoto, Proc. Int. Workshop on Strangeness Nuclear Physics, Seoul (World Scientific 1999), p. 116.

[4] H. Bandō, T. Motoba and Y. Yamamoto, Phys. Rev. **C31** 265 (1985).

[5] A. Likar, M. Rosina and B. Povh, Z. Phys. **A324** 35 (1986).

[6] T. Yamazaki
Proc. KEK Int. Workshop on Nuclear Physics in the GeV region, KEK Report 84-20(1984) p.3.

[7] C.B. Dover
Proc. Int. Symp. on medium energy physics, Beijing, World Scientific 1987) p.257.

[8] Th.A. Rijken *et al.*, Nucl. Phys.**547** (1992) 245c.

[9] Y. Yamamoto and H. Bando, Prog. Theor. Phys. Suppl.**81** (1985) 9.

[10] O. Hashimoto, Hyperfine Interactions **103** (1996) 245.

[11] T. Nagae, Nucl. Phys. **A670** (2000) 269c-272c.

[12] O. Hashimoto *et al.* Il Nuovo Cimento **102** 679 (1989).

[13] T. Fukuda *et al.*, Nucl. Instr. Meth. **A361** (1995) 485.

[14] T. Hasegawa *et al.*, Phys. Rev. Lett. **74** (1995) 224.

[15] T. Tamura *et al.*, Phys. Rev. Lett. **84** (2000) 5963.

[16] H. Tamura, Talk at HYP2000, October 21-26, 2000, Torino, Italy.

[17] T. Kishimoto, Talk at HYPJLAB99, December 5-7, 2000, Hampton, Virginia, USA.

[18] T. Motoba, H. Bandō, R. Wünsch and J. Zofka, Phys. Rev. **C38** 1322 (1988).

[19] C.B. Dover, L. Ludeking and G.E. Walker, Phys. Rev. **C22** 2073 (1980).

[20] H. Bandō and T. Motoba, Prog. Theor. Phys. **76** 1321 (1986).

[21] T. Motoba, M. Sotona and K. Itonaga, Prog. Thor. Phys. Suppl. No. 117 (1994) 123.

[22] M. Sotona *et. al.*, Proceedings of Mesons and Light Nuclei '98, p. 207. 1998.

[23] E. Hungerford, Talk at HYP2000, October 21-26, 2000, Torino, Italy.

[24] A. Gal, Proc. 23rd INS symp., p.23, Eds. S. Sugimoto and O. Hashimoto (University Academy 1995)

[25] T. Motoba *et. al.* Nucl. Phys. **A639** (1998) 135c.

[26] T. Motoba, Private communication, 1997.

Figures

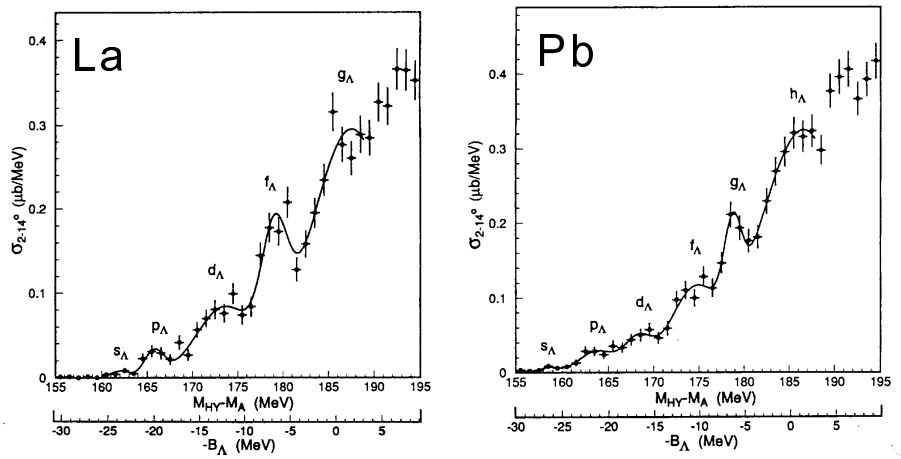

Figure 1: Excitation energy spectrum of ${}^{139}_{\Lambda}$La and ${}^{208}_{\Lambda}$Pb measured with the SKS spectrometer of KEK-PS by the (π^+, K^+) reaction.

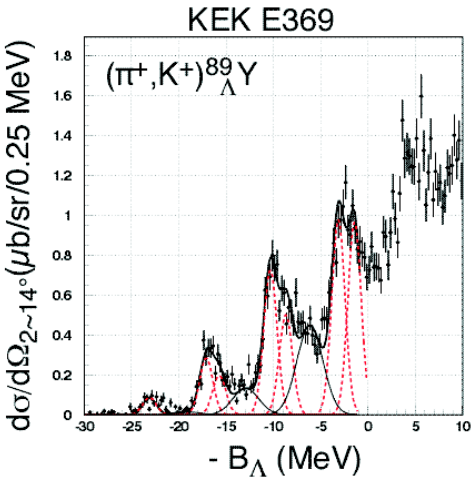

Figure 2: Excitation energy spectrum of ${}^{89}_{\Lambda}$Y measured with the SKS spectrometer of KEK-PS by the (π^+, K^+) reaction.

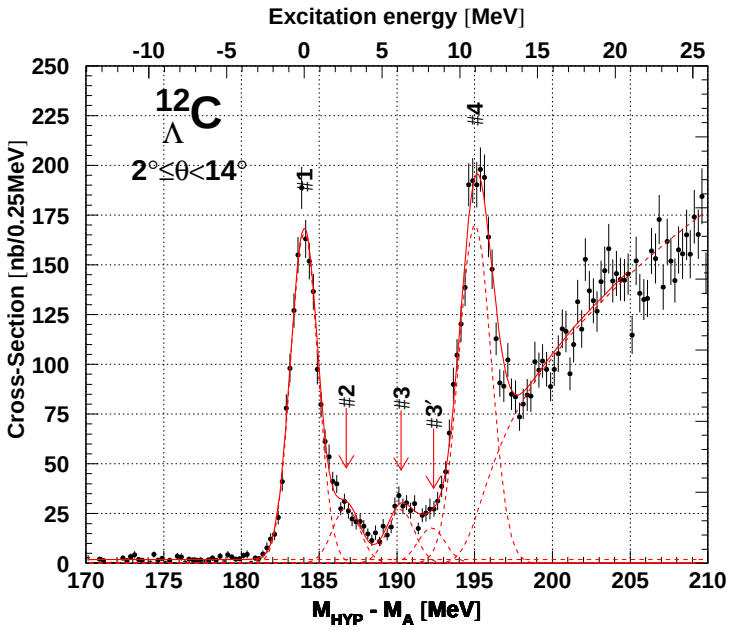

Figure 3: Excitation energy spectrum of $^{12}_{\Lambda}$C measured with the SKS spectrometer of KEK-PS by the (π^+, K^+) reaction.

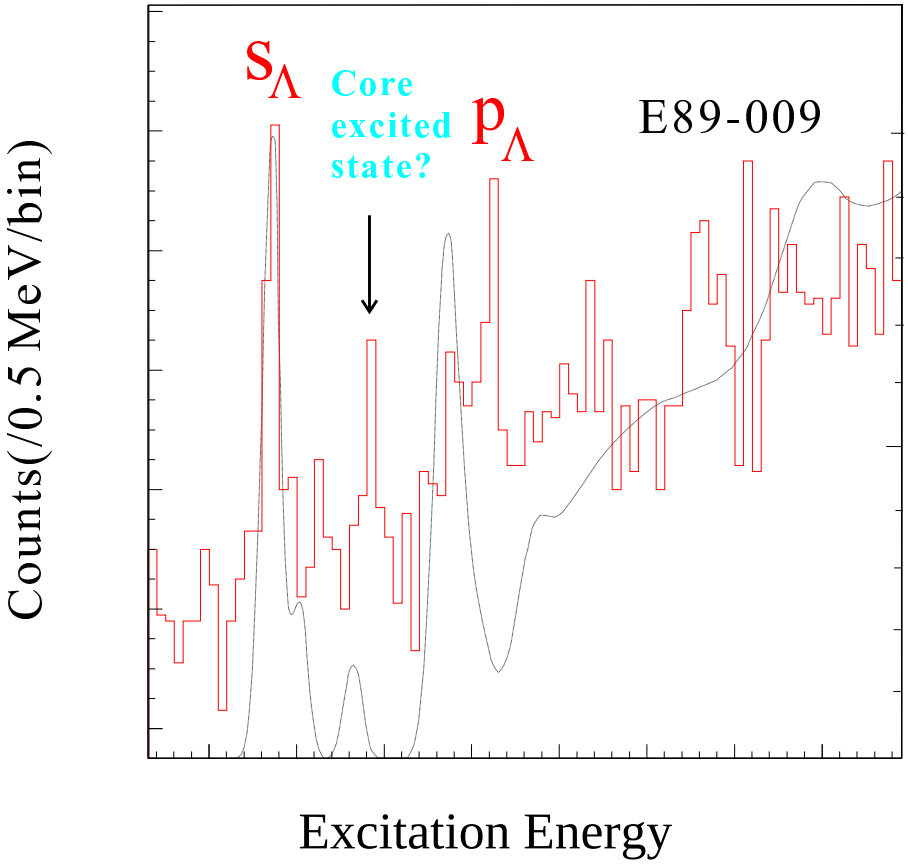

Figure 4: Excitation energy spectrum measured in the E89-009 experiment. Solid line shows the result of Motoba's calculation.

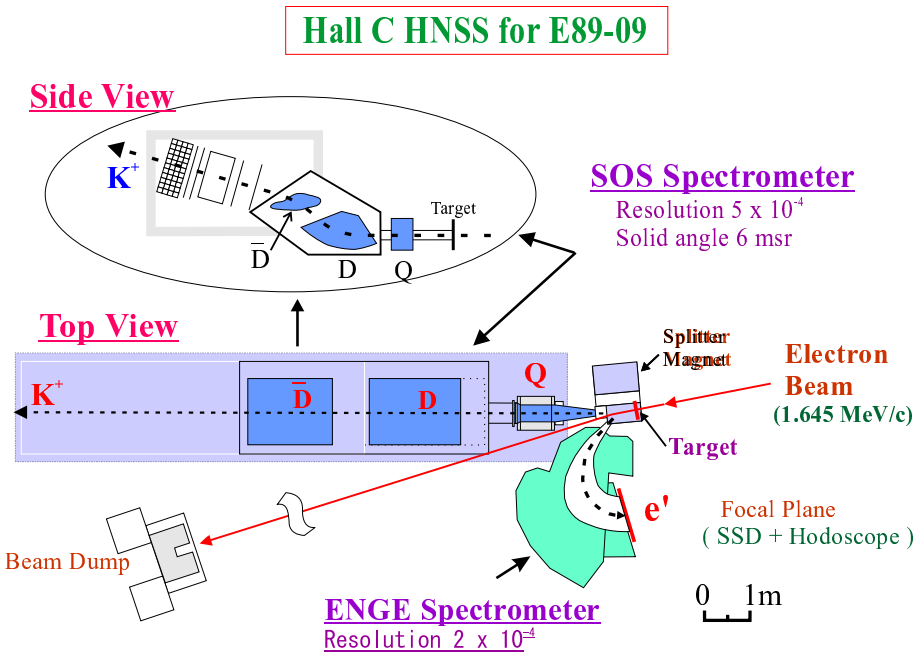

Figure 5: A schematic view of the E89-009 setup.

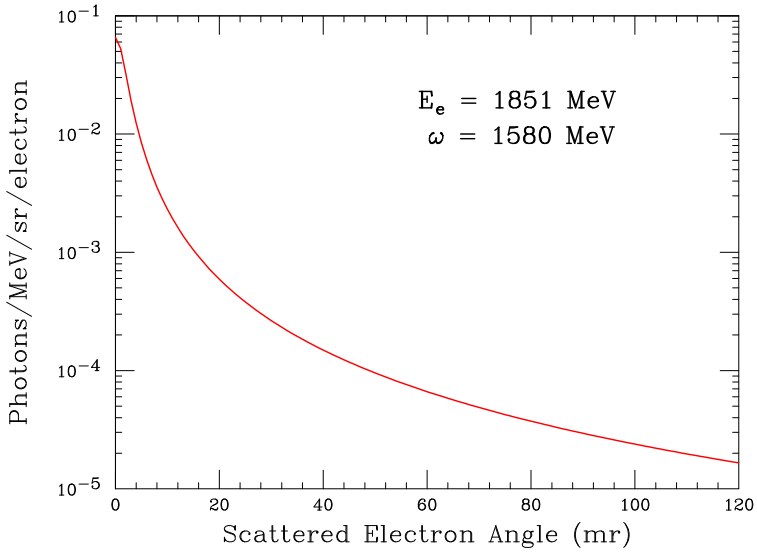

Figure 6: Angular distribution of virtual photons with the ^{12}C target

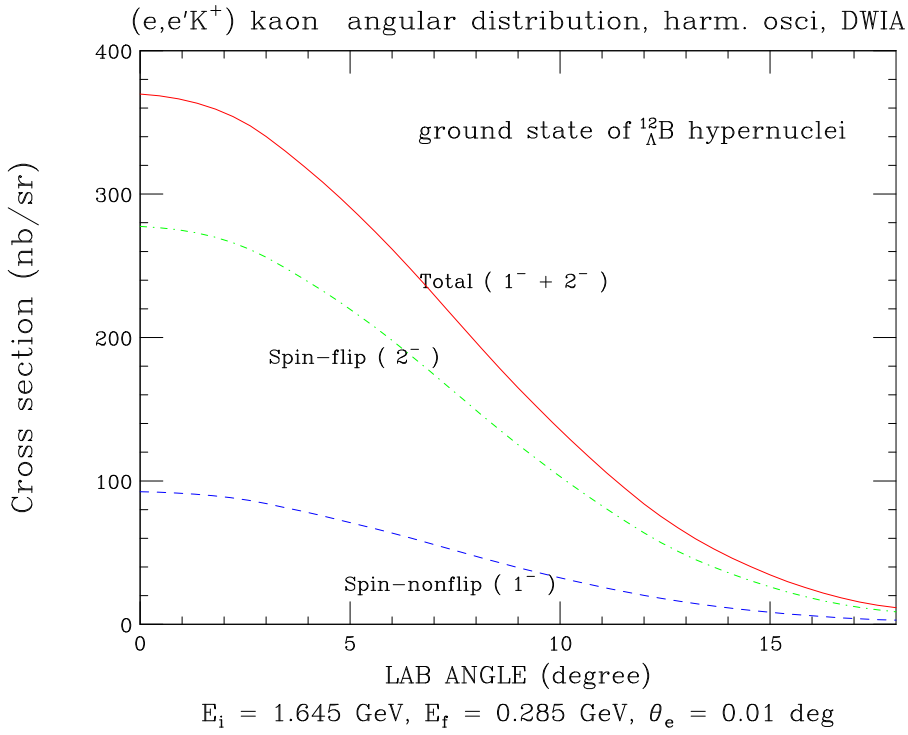

Figure 7: Angular distribution of kaon in the ^{12}C(e,e'K$^+$)$^{12}_{\Lambda}$B reaction.

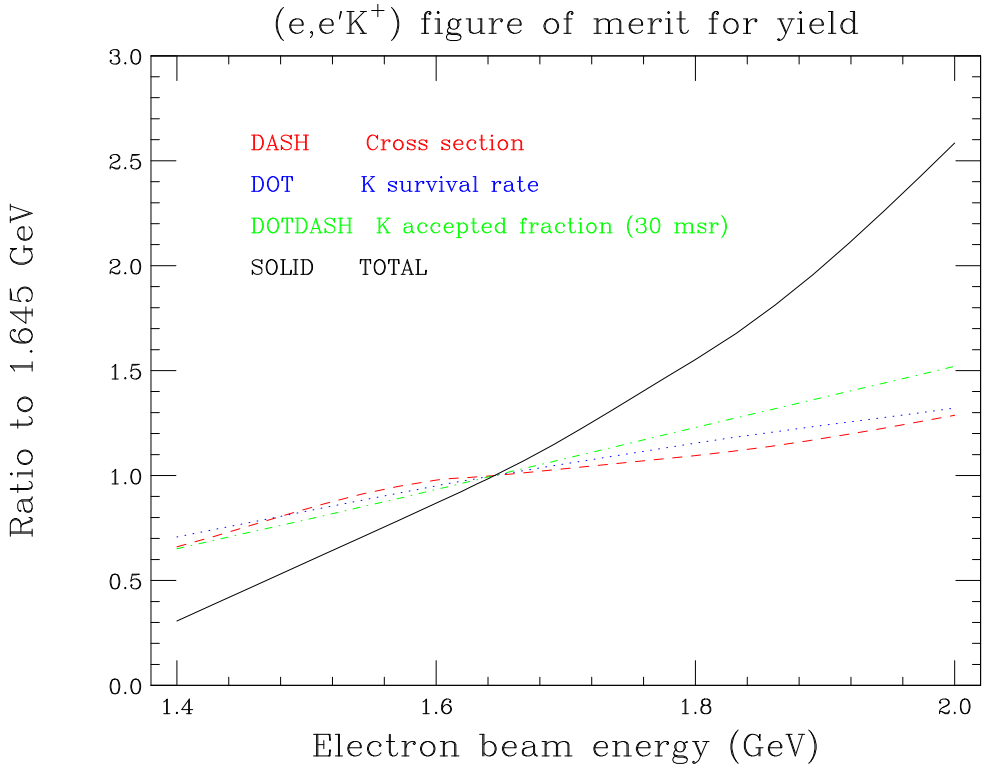

Figure 8: Hypernuclear yield of $^{12}_{\Lambda}B_{gr}$ as a function of the beam energy assuming scattered electrons are measured at E_e = 0.285 GeV.

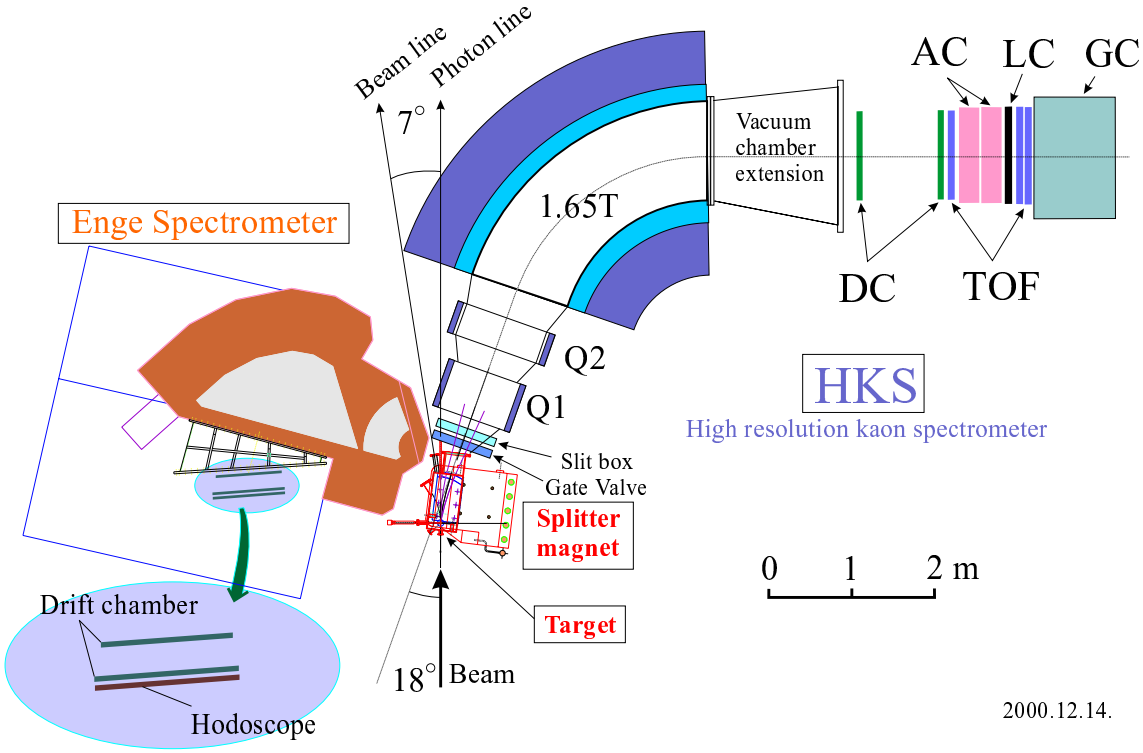

Figure 9: Plan view of the high-resolution kaon spectrometer (HKS) and Enge spectrometer for the proposed experiment.

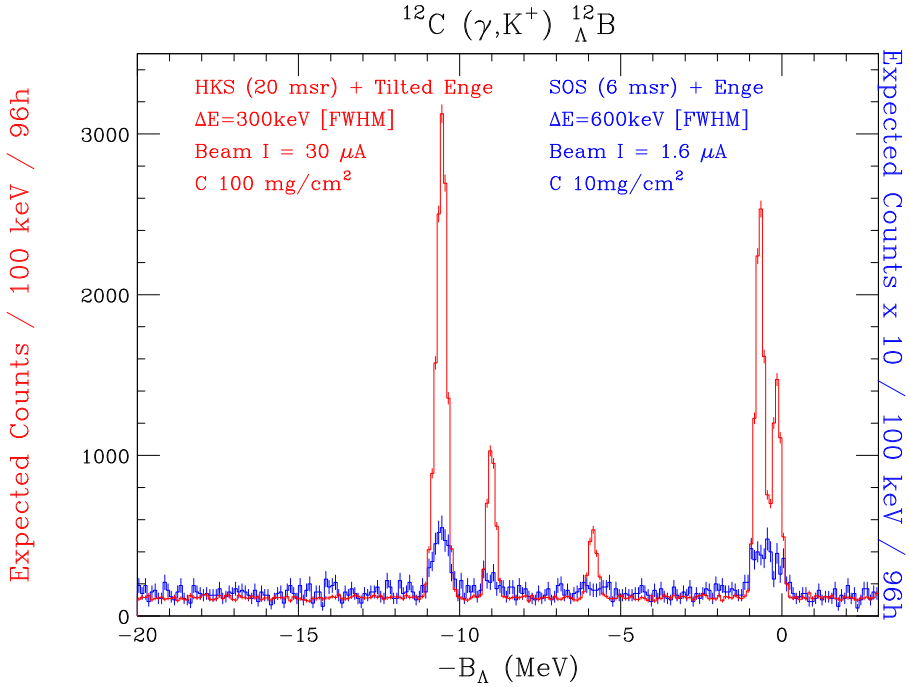

Figure 10: Simulated spectrum of the ^{12}C(e,e'K$^+$)$^{12}_{\Lambda}$B reaction to be observed by the HKS in the proposed beam hours.

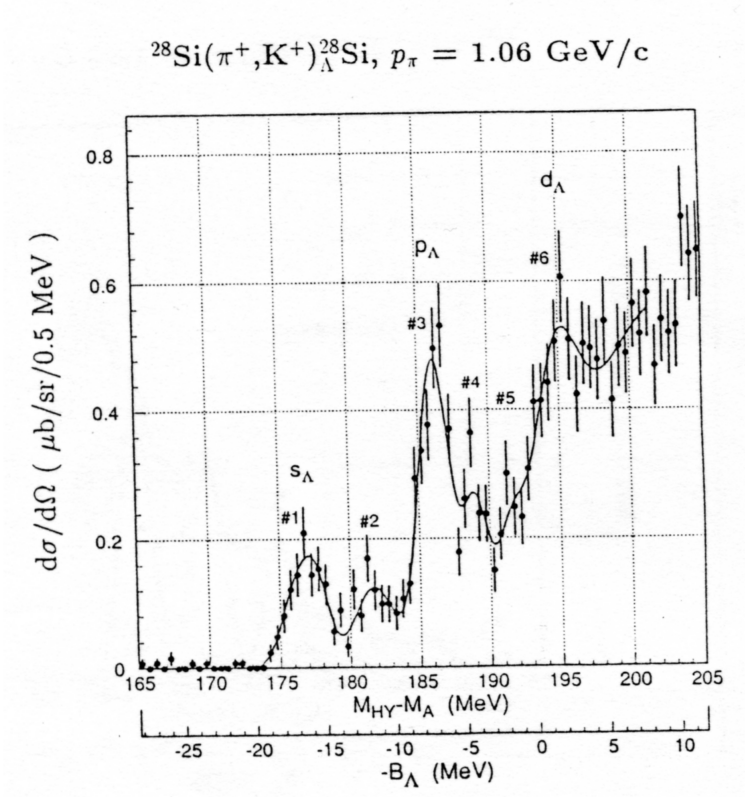

Figure 11: Excitation energy spectrum of $^{28}_{\Lambda}$Si measured with the SKS spectrometer of KEK-PS by the (π^+, K^+) reaction.

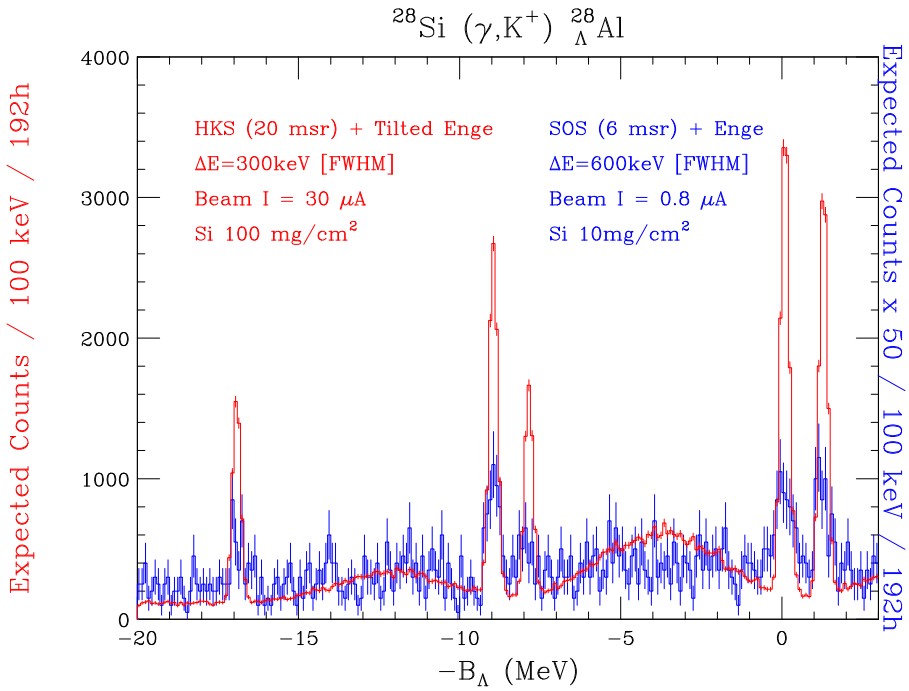

Figure 12: Simulated spectrum of the ^{28}Si(e,e'K$^+$)$^{28}_{\Lambda}$Al reaction to be observed by the HKS in the proposed beam hours.

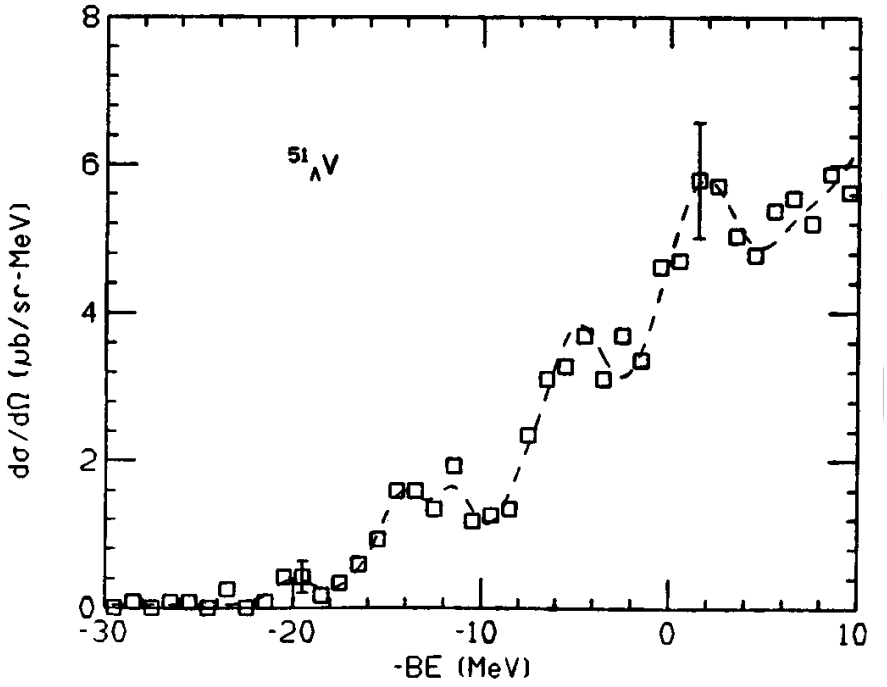

Figure 13: Excitation spectrum of the ^{51}V(π^+,K$^+$)$^{51}_{\Lambda}$V reaction measured at BNL [1].

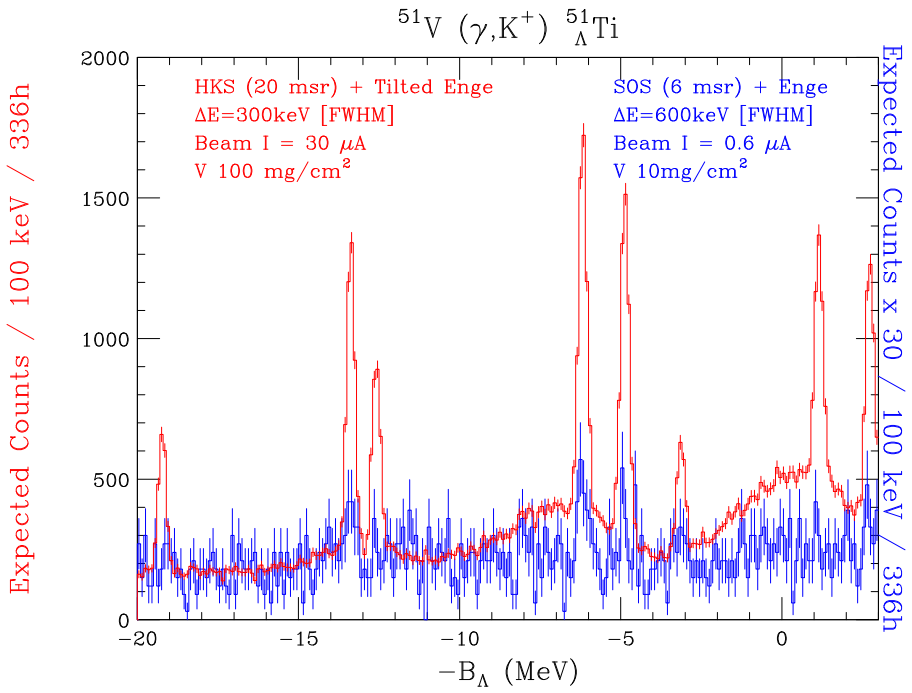

Figure 14: Simulated spectrum of the ^{51}V(e,e'K$^+$)$^{51}_{\Lambda}$Ti reaction to be observed by the HKS in the proposed beam hours.

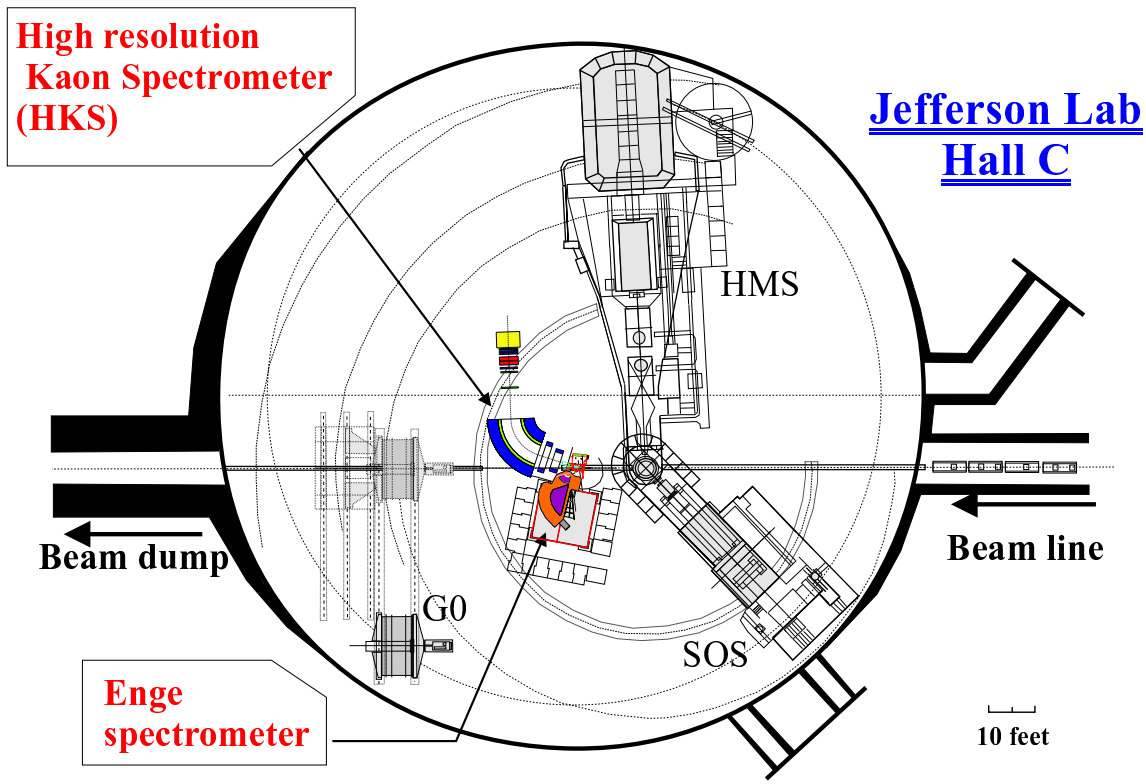

Figure 15: Expected Hall C setup of the HKS and Enge spectrometer. The installation can be compatible with the G0 setup.

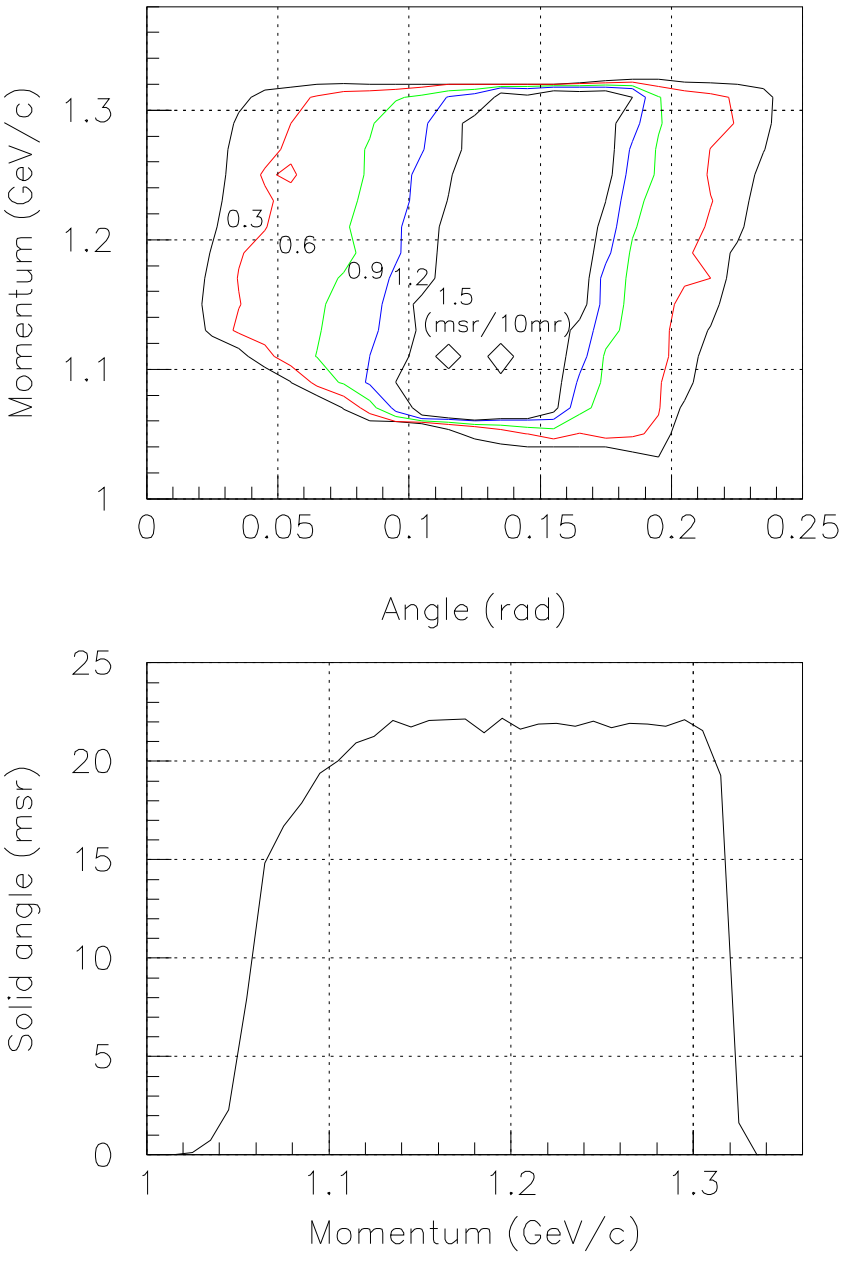

Figure 16: Acceptance of the HKS spectrometer with the splitter installed.

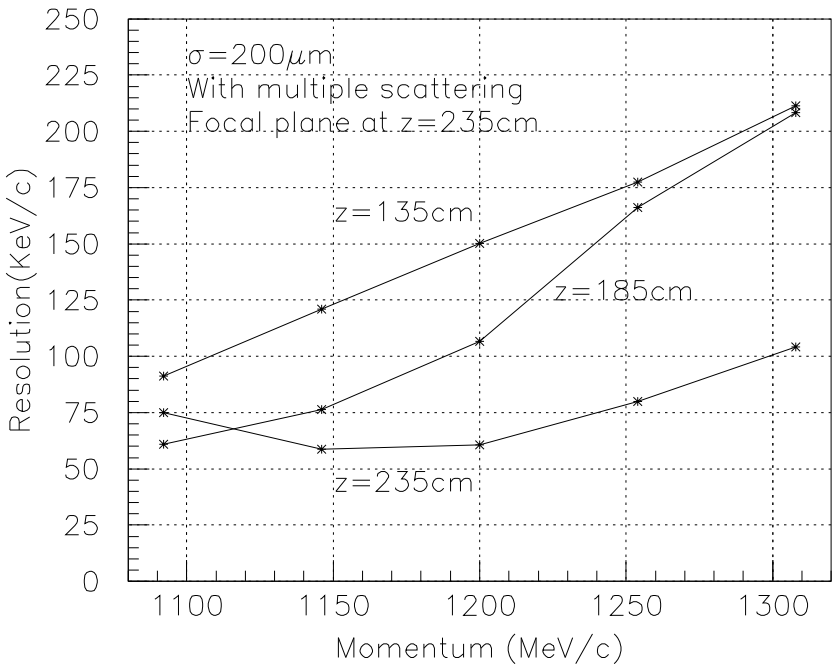

Figure 17: Resolution of the HKS spectrometer.

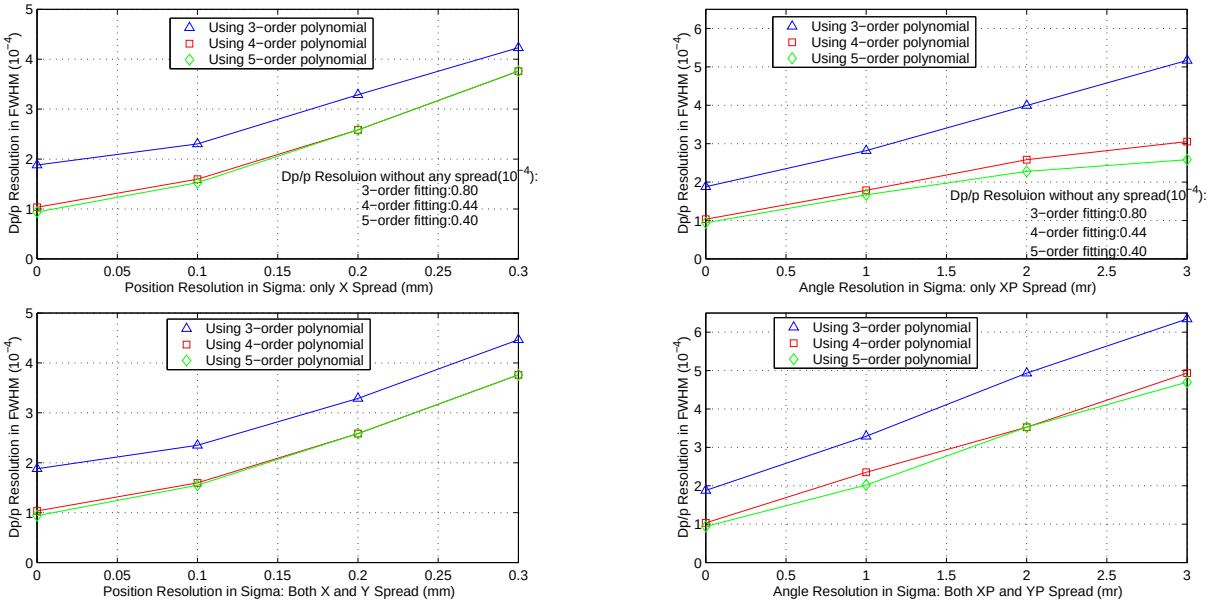

Figure 18: Energy resolution of the Enge spectrometer for electrons.